

Photooxidation of Platinum(II) Diimine Dithiolates

William B. Connick and Harry B. Gray*

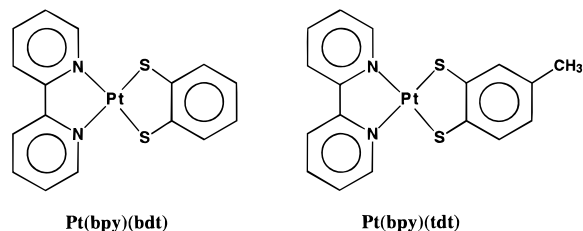
Contribution from the Beckman Institute, California Institute of Technology, Pasadena, California 91125

Received July 16, 1997[⊗]

Abstract: The violet color of Pt(bpy)(bdt) (bpy = 2,2'-bipyridine; bdt = 1,2-benzenedithiolate) is due to a Pt/S → diimine charge-transfer transition; the emission originates from the corresponding triplet state ($\tau = 460$ ns). Photochemical oxidation of Pt(bpy)(bdt) occurs in the presence of oxygen in *N,N*-dimethylformamide, acetonitrile, or dimethyl sulfoxide solution; the reaction has been investigated by ¹H NMR and UV–visible absorption spectroscopy. Singlet oxygen produced by energy transfer from the excited complex is implicated as the active oxygen species, in sequential formation of sulfinate, Pt(bpy)(bdtO₂), and disulfinate, Pt(bpy)(bdtO₄), products. Both products have been characterized by X-ray crystallography. The rate of photooxygenation is strongly dependent on water concentration, and transient absorption spectra are consistent with the formation of at least one intermediate. As a whole, our data suggest that the photooxidation chemistry of platinum(II) diimine dithiolates is similar to that of organic sulfides.

Introduction

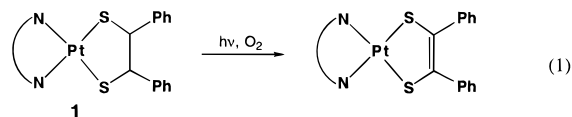
Platinum(II) complexes containing dithiolate (donor) and diimine (acceptor) ligands are intensely colored, owing to an absorption that has been attributed to a Pt/S → diimine charge-transfer (CT) transition.^{1–5} In 1989, Eisenberg and co-workers⁵ discovered that certain of these complexes luminesce in fluid solution (e.g., Pt(bpy)(tdt): $\lambda_{\text{max}} = 735$ nm; $\tau = 291$ ns; tdt = 3,4-toluenedithiolate),¹ probably from a ³CT excited state.



In extensive investigations, Srivastava and co-workers⁶ demonstrated that literally dozens of platinum(II) and palladium(II) diimine complexes sensitize the formation of singlet oxygen (¹O₂) from ground-state oxygen (³O₂). In the course of this work, it was established that complexes with thiolate ligands undergo photoinduced decomposition in the presence of oxygen.^{7–10}

In 1996, the photooxidation chemistry of two platinum(II) diimine dithiolate complexes [Pt(dbbpy)(dpdt) (**1**) and Pt(dbbpy)(edt) (**2**) (dbbpy = 4,4'-di-*tert*-butyl-2,2'-bipyridine; dpdt = *meso*-1,2-diphenyl-1,2-ethanedithiolate; edt = 1,2-ethanedithiolate)] was examined by Schanze and co-workers.¹¹ The reactivity of **2** is similar to that of compounds studied by Srivastava; irradiation of an air-saturated solution results in a gradual bleaching of the CT band (466 nm) and other visible charge-transfer features. In contrast, irradiation of an air-saturated solution of **1** causes bleaching of the CT band (466 nm) accompanied by the emergence of a new band at longer wavelength (582 nm). This unusual behavior appears to suggest a novel type of photoreactivity for platinum(II) diimine dithiolate complexes. Schanze performed a thorough analysis of kinetics and quenching data that largely confirms that these reactions also involve singlet oxygen.

The photoproducts of the reactions of **1** and **2** with oxygen have not been fully characterized. However, for the reaction involving **1**, the UV–visible absorption and ¹H NMR spectra as well as the mass spectrum are consistent with loss of two H atoms to form the dithiolene adduct.¹¹ In contrast, the products



of the reaction involving **2** are insufficiently soluble for NMR studies, although the mass spectrum suggests that the reaction involves addition of oxygen to the metal complex.

In order to investigate the photoreactivity associated with platinum(II) diimine dithiolate complexes such as **2**, we have prepared C_{2v} Pt(bpy)(bdt) (bdt = 1,2-benzenedithiolate). This violet-colored complex undergoes a series of oxygenation reactions when irradiated with visible light in the presence of oxygen. The high symmetry of this system has greatly

[⊗] Abstract published in *Advance ACS Abstracts*, November 1, 1997.

(1) Cummings, S. D.; Eisenberg, R. *J. Am. Chem. Soc.* **1996**, *118*, 1949.

(2) Bevilacqua, J. M.; Eisenberg, R. *Inorg. Chem.* **1994**, *33*, 1886.

(3) Zuleta, J. A.; Bevilacqua, J. M.; Proserpio, D. M.; Harvey, P. D.; Eisenberg, R. *Inorg. Chem.* **1992**, *31*, 2396.

(4) Zuleta, J. A.; Burberry, M. S.; Eisenberg, R. *Coord. Chem. Rev.* **1990**, *97*, 47.

(5) Zuleta, J. A.; Chesta, C. A.; Eisenberg, R. *J. Am. Chem. Soc.* **1989**, *111*, 8916.

(6) Anbalagan, V.; Srivastava, T. S. *J. Photochem. Photobiol., A: Chem.* **1995**, *89*, 113. Anbalagan, V.; Srivastava, T. S. *J. Photochem. Photobiol., A: Chem.* **1994**, *77*, 141. Anbalagan, V.; Srivastava, T. S. *Polyhedron* **1994**, *13*, 291. Kamath, S. S.; Uma, V.; Srivastava, T. S. *Inorg. Chim. Acta* **1989**, *166*, 91. Anbalagan, V.; Srivastava, T. S. *J. Photochem. Photobiol., A: Chem.* **1992**, *66*, 345. Kamath, S. S.; Srivastava, T. S. *J. Photochem. Photobiol., A: Chem.* **1990**, *52*, 83. Shukla, S.; Kamath, S. S.; Srivastava, T. S. *J. Photochem. Photobiol., A: Chem.* **1988**, *44*, 143. Kumar, L.; Puthraya, K. H.; Srivastava, T. S. *Inorg. Chim. Acta* **1984**, *86*, 173.

(7) Paul, A. K.; Venkatesan, R.; Srivastava, T. S. *J. Photochem. Photobiol., A: Chem.* **1991**, *56*, 399.

(8) Kamath, S. S.; Shukla, S.; Srivastava, T. S. *Bull. Chem. Soc. Jpn.* **1991**, *64*, 1351. Shukla, S.; Kamath, S. S.; Srivastava, T. S. *J. Photochem. Photobiol., A: Chem.* **1989**, *47*, 287. Shukla, S.; Kamath, S. S.; Srivastava, T. S. *J. Photochem. Photobiol., A: Chem.* **1989**, *50*, 199.

(9) Puthraya, K. H.; Srivastava, T. S. *J. Ind. Chem. Soc.* **1985**, *62*, 843.

(10) Puthraya, K. H.; Srivastava, T. S. *Polyhedron* **1985**, *4*, 1579.

(11) Zhang, Y.; Ley, K. D.; Schanze, K. S. *Inorg. Chem.* **1996**, *35*, 7102.

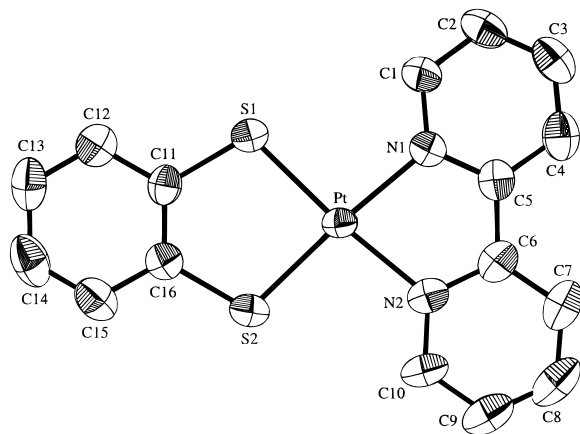


Figure 1. ORTEP diagram with 50% probability ellipsoids showing the geometry of the Pt(bpy)(bdt) molecule. H atoms are not shown.

facilitated characterization of the photoproducts by ^1H NMR spectroscopy. Thus, for the first time, we report the identity of two of these photoproducts and their crystal structures. In addition, at least one intermediate along the photooxidation pathway has been observed by time-resolved transient absorption spectroscopy.

Results and Discussion

Molecular Structure. The Pt(bpy)(bdt) complex, including the numbering system, is drawn in Figure 1; selected distances and angles are given in Table 2. The molecule is slightly bowed with an average deviation of 0.06(4) Å per atom for a best-fit plane defined by the positions of the atoms. Distances and angles in the ligands are normal.

The Pt–N bond lengths (2.050(4), 2.049(5) Å) are within the range of those observed for other platinum(II) diimine complexes with dithiolate (2.03–2.06 Å)^{12–14} and cyanide ligands (e.g., Pt(bpy)(CN)₂, 2.059(5) Å),^{15–20} but they are significantly longer than found for the red and yellow forms of Pt(bpy)Cl₂ (2.009(6) and 2.01(1) Å).²¹ The Pt–S distances (2.244(2), 2.250(2) Å) are characteristically short, suggesting a strong Pt–S interaction. The Pt–S distances are similar to those of other platinum(II) diimine dithiolates¹² (e.g., Pt(bpm)(mnt), 2.245(3), 2.254(2), mnt = maleonitriledithiolate, bpm = 2,2'-bipyrimidine;¹⁴ Pt(dmbpy)(met), 2.245(2), 2.244(2) Å,²² met = *cis*-1,2-dicarbomethoxyethylene-1,2-dithiolate, dmbpy = 4,4'-dimethyl-2,2'-bipyridine), but they are shorter than found for complexes with phosphine ligands (Pt(dppe)(mnt), 2.303(2) and 2.296(2) Å, dppe = 1,2-bis(diphenylphosphino)ethane).^{13,22}

(12) Zuo, J.-L.; Xiong, R.-G.; You, X.-Z.; Huang, X.-Y. *Inorg. Chim. Acta* **1995**, *237*, 177.

(13) Bevilacqua, J. M.; Eisenberg, R. *Inorg. Chem.* **1994**, *33*, 2913.

(14) Matsubayashi, G.; Yamaguchi, Y.; Tanaka, T. *J. Chem. Soc., Dalton Trans.* **1988**, 2215.

(15) Kato, M.; Sasano, K.; Kosuge, C.; Yamazaki, M.; Yano, S.; Kimura, M. *Inorg. Chem.* **1996**, *35*, 116.

(16) Connick, W. B.; Henling, L. M.; Marsh, R. E. *Acta Crystallogr.* **1996**, *B52*, 817.

(17) Biedermann, J.; Gliemann, G.; Klement, U.; Range, K.-J.; Zabel, M. *Inorg. Chim. Acta* **1990**, *171*, 35.

(18) Biedermann, J.; Gliemann, G.; Klement, U.; Range, K.-J.; Zabel, M. *Inorg. Chem.* **1990**, *29*, 1884.

(19) Biedermann, J.; Gliemann, G.; Klement, U.; Range, K.-J.; Zabel, M. *Inorg. Chim. Acta* **1990**, *169*, 63.

(20) Che, C.-M.; He, L.-Y.; Poon, C.-K.; Mak, T. C. M. *Inorg. Chem.* **1989**, *28*, 3081.

(21) Osborn, R. J.; Rogers, D. *J. Chem. Soc., Dalton Trans.* **1974**, 1002. Canty, A. J.; Skelton, B. W.; Traill, P. R.; White, A. H. *Aust. J. Chem.* **1992**, *45*, 417. Connick, W. B.; Henling, L. M.; Marsh, R. E.; Gray, H. B. *Inorg. Chem.* **1996**, *35*, 6261.

(22) Bevilacqua, J. M.; Zuleta, J. A.; Eisenberg, R. *Inorg. Chem.* **1994**, *33*, 258.

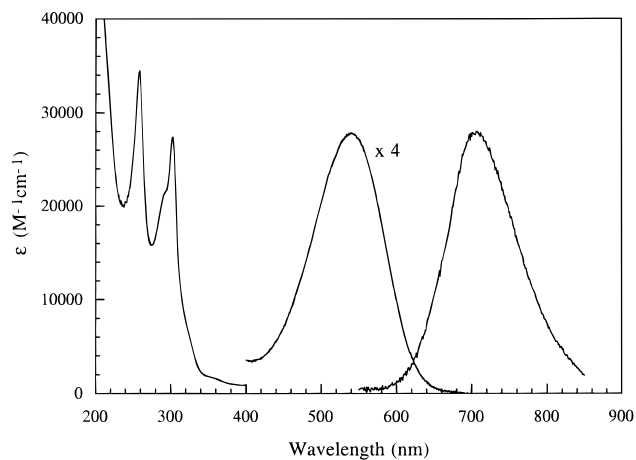


Figure 2. Absorption and uncorrected emission spectra for Pt(bpy)(bdt) in acetonitrile. (The corrected emission maximum occurs near 750 nm.)

Electronic Structure. As expected, the UV–visible absorption spectrum of Pt(bpy)(bdt) is similar to spectra of Pt(diimine)-(tdt) complexes (Figure 2). Two solvent-insensitive, intense narrow bands are observed in the UV region (acetonitrile: 260 nm, $\epsilon = 34\,500\text{ M}^{-1}\text{ cm}^{-1}$; 310 nm, $\epsilon = 27\,400\text{ M}^{-1}\text{ cm}^{-1}$). In analogy to related systems,²³ the lower energy feature is assigned to the bipyridyl localized $\pi \rightarrow \pi_1^*$ transition; the higher energy band lies very near the $\pi \rightarrow \pi_2^*$ transition observed in the spectra of other Pt(bpy)X₂ complexes ($\sim 250\text{ nm}$).²⁴ The high intensities of these bands indicate that transitions associated with the bdt ligand also overlap this region. At longer wavelengths, a shoulder is resolved near 350 nm ($\epsilon = 1850\text{ M}^{-1}\text{ cm}^{-1}$); in chloroform, the shoulder shifts to $\sim 363\text{ nm}$. The energy, intensity, and solvent sensitivity are consistent with a $^1\text{MLCT}$ -[$d \rightarrow \pi^*(\text{bpy})$] transition. It is striking that this band occurs in the same region (330–450 nm) as the $d\pi(\text{Pt}) \rightarrow \pi^*(\text{diimine})$ transition in the spectra of Pt(diimine)X₂ complexes with innocent ligands.^{23–26}

A very broad and solvent sensitive band occurs at longer wavelengths (acetonitrile λ_{max} , nm (ϵ , $\text{M}^{-1}\text{ cm}^{-1}$), 542 (6960); DMF, 557 (7080); chloroform, 600). A similar band has been observed in the spectra of numerous platinum(II) dithiolate complexes and can be described as CT, coupled to the intense $d \rightarrow p$ transitions of platinum and involving transfer of electron density from the dithiolate ligand to the diimine ligand. The band shifts dramatically to lower energy in less polar solvents, suggesting considerable charge-transfer character; this large negative solvatochromism indicates a polar ground state and a nonpolar excited state.¹ Evidence of ligand participation²⁷ comes from diffuse reflectance measurements of Pt(bpy)(bdt) that reveal vibronic structure with 1100–1600 cm^{-1} spacings. Resonance Raman studies of related nickel and palladium compounds also support this assignment.²⁸

Like many platinum(II) diimine dithiolate complexes, Pt(bpy)(bdt) is luminescent in room-temperature fluid solution (Figure 2). The excited-state lifetime is concentration dependent (the lifetime decreases as the concentration of complex in solution is increased), indicating self-quenching. A Stern–Volmer

(23) Miskowski, V. M.; Houlding, V. H. *Inorg. Chem.* **1989**, *28*, 1529.

(24) Gidney, P. M.; Gillard, R. D.; Heaton, B. T. *J. Chem. Soc., Dalton Trans.* **1973**, 132.

(25) Textor, V. M.; Oswald, H. R. *Z. Anorg. Allg. Chem.* **1974**, *407*, 244.

(26) Miskowski, V. M.; Houlding, V. H.; Che, C.-M.; Wang, Y. *Inorg. Chem.* **1993**, *32*, 2518.

(27) Kober, E. M.; Meyer, T. *J. Inorg. Chem.* **1982**, *21*, 3967; Kober, E. M.; Meyer, T. *J. Inorg. Chem.* **1984**, *23*, 3877.

(28) Wootton, J. L.; Zink, J. I. *J. Phys. Chem.* **1995**, *99*, 7251.

analysis shows that the intrinsic lifetime of the excited state is 460 ns in acetonitrile, and the quenching rate constant ($k_q = 9.5 \times 10^9 \text{ M}^{-1} \text{ s}^{-1}$) is near the diffusion limit; for chloroform solution, the intrinsic lifetime is 560 ns ($k_q = 4 \times 10^9 \text{ M}^{-1} \text{ s}^{-1}$). It is likely that the self-quenching reaction involves formation of an excimer, as reported for other platinum(II) diimine systems.^{29–31}

The emission band overlaps the low-energy tail of the absorption system and has a similar solvent dependence. In addition, a distinct shoulder is resolved in the solid-state emission spectrum; it is shifted 1040 cm^{-1} to lower energy of the parent peak (730 nm), indicating the involvement of the bipyridyl ligand in the electronic transition. Moreover, the long excited-state lifetime is consistent with a spin-forbidden process. In analogy to studies of related complexes,^{1,2,4,5,13,32–35} the emission is proposed to originate from a CT state with triplet character. Although corresponding triplet absorption features have not been resolved in the spectra of platinum(II) diimine dithiolate complexes, they are believed to be buried in the low-energy tail of the absorption band.¹ From the overlap of the emission spectrum with the absorption spectrum, it is apparent that the gap between these singlet and triplet states is small ($\sim 1000 \text{ cm}^{-1}$). In fact, it appears that this gap is smaller than found for splitting of unimolecular singlet–triplet MLCT states of platinum diimine complexes ($3000\text{--}4000 \text{ cm}^{-1}$),^{26,36} this situation is consistent with spin-orbit coupling with the Pt as well as an excited state involving large spatial separation of the unpaired electrons (as expected for a CT state).³⁷

Electrochemical measurements as well as spectroelectrochemical and electron paramagnetic resonance data³⁸ also are consistent with a charge-separated excited state. From these data, it is evident that in the excited state Pt(bpy)(bdt) is a powerful reductant and a relatively strong oxidant.

(29) Wan, K.-T.; Che, C.-M.; Cho, K.-C. *J. Chem. Soc., Dalton Trans.* **1991**, 1077.

(30) Kunkely, H.; Vogler, A. *J. Am. Chem. Soc.* **1990**, *112*, 5625.

(31) An excimer and its corresponding emission have not been directly observed; however, we note that this emission is likely to occur at wavelengths outside the detection limits of our instrument ($> 850 \text{ nm}$). Interestingly, Pt(bpy)(tdt) and other tdt complexes do not exhibit self-quenching.¹ The methyl group on tdt apparently reduces the association constant.

(32) Vogler, A.; Kunkely, H. *J. Am. Chem. Soc.* **1981**, *103*, 1559.

(33) Cummings, S. D.; Eisenberg, R. *Inorg. Chem.* **1995**, *34*, 3396.

(34) Zuleta, J. A.; Bevilacqua, J. M.; Eisenberg, R. *Coord. Chem. Rev.* **1991**, *111*, 237.

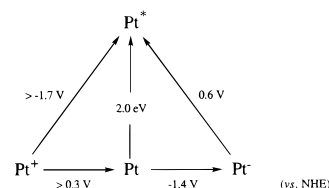
(35) Zuleta, J. A.; Bevilacqua, J. M.; Rehm, J. M.; Eisenberg, R. *Inorg. Chem.* **1992**, *31*, 1332.

(36) Connick, W. B.; Miskowski, V. M.; Houlding, V. H.; Gray, H. B. Manuscript in preparation.

(37) An alternative interpretation is that the intense absorption band corresponds to a transition to a strongly spin-orbit-coupled triplet CT state, and the emission originates from a more weakly coupled spin-orbit state. This situation is similar to that observed for the MLCT transitions of $\text{Pt}(\text{CN})_4^{2-}$ (Isci, H.; Mason, W. R. *Inorg. Chem.* **1975**, *14*, 905. Piepho, S. B.; Schatz, P. N.; McCaffery, A. J. *J. Am. Chem. Soc.* **1969**, *91*, 5994. Cowman, C. D.; Gray, H. B. *J. Am. Chem. Soc.* **1976**, *15*, 2823).

(38) The complex exhibits chemically reversible half-electron oxidations at 0.40 and 0.70 V and a one-electron reduction at -1.31 V vs AgCl/Ag in 1.0 M KCl. A second reduction at -1.99 V is irreversible. The two half-electron oxidations are not fully understood; though they are consistent with dimer formation, electrode surface adsorption prevented complete characterization of these processes. The spectrum of the reduced species exhibits features characteristic of bpy anion radical, confirming that the LUMO is predominantly ligand-centered (Klein, A.; Kaim, W. *Organometallics* **1995**, *14*, 1176. Collison, D.; Mabbs, F. E.; McInnes, E. J. L.; Taylor, K. J.; Welch, A. J.; Yellowlees, L. J. *J. Chem. Soc., Dalton Trans.* **1995**, 329. Braterman, P. S.; Song, J. I.; Wimmer, F. M.; Wimmer, S.; Kaim, W.; Klein, A.; Peacock, R. D. *Inorg. Chem.* **1992**, *31*, 5084.). Spectra of the one-electron oxidized species obtained by electrochemical methods or chemical titration are identical and no evidence of oligomerization was found. The frozen solution EPR spectrum (1:1 Ce(IV):Pt(bpy)(bdt)) of the oxidized complex gave a g value of 2.0035(2); the signal was slightly broad (80 G), though no anisotropy was observed (Hill, M. G.; Connick, W. B. Unpublished results.).

Scheme 1



Interestingly, Pt(bpy)(bdt) reacts thermally with CH_3I . ^1H NMR and UV–visible absorption spectra are consistent with thiolate methylation.³⁹ In chloroform solution, Pt(bpy)(tdt) is photochemically unstable,³² as is the bdt complex; upon irradiation at $\lambda > 450 \text{ nm}$, the CT absorption band loses intensity, and a shoulder emerges near 390 nm. Vogler and Kunkely³² have proposed that the tdt complex reacts with CHCl_3 to give Cl^- and the $\cdot\text{CHCl}_2$ radical, with subsequent steps leading to the observed degradation. Our results indicate that sulfur is a likely site for attack.³⁹

Photochemical Oxygenation. Violet-colored air-saturated solutions of Pt(bpy)(bdt) gradually turn yellow in the presence of visible light. Both oxygen and light are necessary for this transformation, and the reaction ceases when either of these reagents is removed. Thus, the photoreaction appears qualitatively similar to those studied by Srivastava^{7–10} and the decomposition of **2** found by Schanze.¹¹ UV–visible absorption spectra recorded while irradiating ($\lambda_{\text{ex}} > 450 \text{ nm}$) an acetonitrile solution of Pt(bpy)(bdt) show that the CT absorption at 542 nm decays as a new band emerges at $\sim 464 \text{ nm}$ (Figure 3). Early in the course of the reaction, the absorbances at 326 and 471 nm do not change (pseudoisobestic points); however, at longer times, spectral changes occur at these wavelengths. This behavior suggests the occurrence of more than one chemical process, and kinetic analyses indicate that these data are well modeled as an $\text{A} \rightarrow \text{B} \rightarrow \text{C}$ type process. Plots of the logarithm of the absorbance at wavelengths where the products do not absorb ($\lambda > 550 \text{ nm}$) are initially linear, as expected for a pseudo-first-order reaction. We observe similar behavior in DMF and DMSO solutions, though the reaction is sluggish in DMSO.⁴⁰

We have followed the course of the reaction by ^1H NMR spectroscopy in DMF- d_7 solution. Irradiation ($\lambda > 400 \text{ nm}$) causes the intensity of the six resonances (6.6–9.2 ppm) in the spectrum of the starting material (A) to gradually decrease while the intensity of 12 new resonances (B, 7–9.8 ppm) with equal integration increases. Further irradiation yields a second product (C), characterized by six new resonances with equal integration

(39) Initially, a DMF solution of Pt(bpy)(bdt) and CH_3I changes color from violet to yellow as the CT band decays, giving rise to a new feature near 458 nm. Early in the course of the reaction, the absorbances at 384 and 478 nm do not change (pseudoisobestic points); however, at longer times, spectral changes occur at these wavelengths, and a new band emerges at 386 nm as the 458 nm band decays. This behavior is consistent with an $\text{A} \rightarrow \text{B} \rightarrow \text{C}$ process. Addition of CH_3I to a solution of Pt(bpy)(bdt) DMSO- d_6 causes the six multiplets between 6.6 and 9.2 ppm to gradually lose intensity with the concomitant emergence of a new pattern of 12 multiplets with equal integration between 7 and 9.2 ppm, as expected for a C_3 product. This result suggests an initial reaction involving thiolate methylation rather than oxidative addition to Pt(II); alkylation of the coordinated sulfur atom of metal-thiolate complexes by alkyl halides has been studied extensively (Burke, J. A. J.; Brink, E. C. J. *Inorg. Chem.* **1969**, *8*, 386. Shoup, J. C.; Burke, J. A. J. *Inorg. Chem.* **1973**, *12*, 1851. Root, M. J.; Deutsch, E. *Inorg. Chem.* **1981**, *20*, 4376. Root, M. J.; Deutsch, E. *Inorg. Chem.* **1984**, *23*, 622.).

(40) The sluggish reactivity in DMSO is not inconsistent with chemical quenching of $^1\text{O}_2$ by the solvent. Though sulfoxides have low reactivities toward $^1\text{O}_2$, the DMSO is in > 1000 -fold excess in our experiments. Alternatively, DMSO may deactivate or react with an intermediate (peroxysulfoxide or superoxide) formed by reaction of the Pt(bpy)(bdt) and $^1\text{O}_2$.

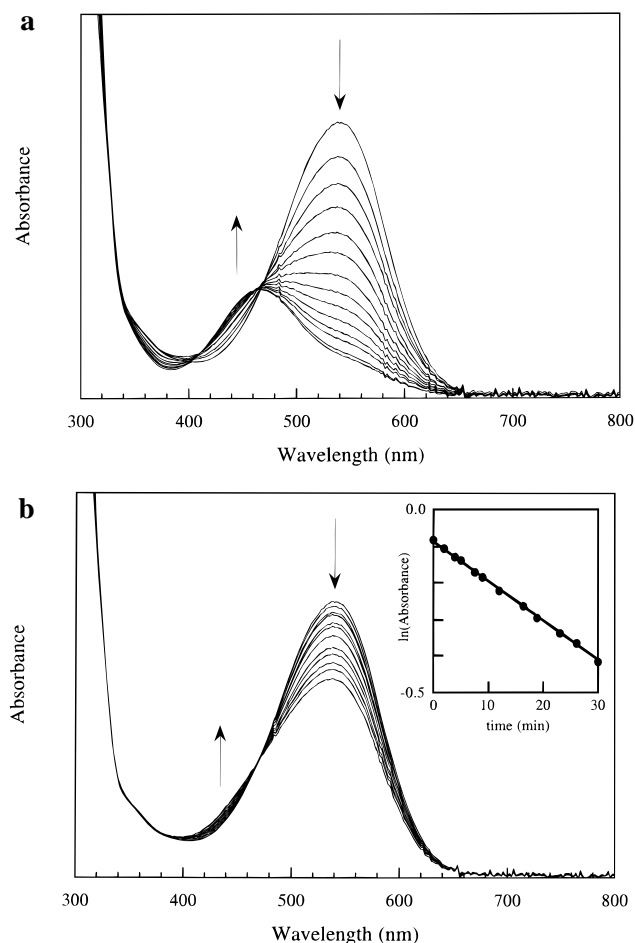


Figure 3. Absorption spectra recorded during the photooxidation of Pt(bpy)(bdt) in acetonitrile while irradiating with a tungsten lamp (150 W; $\lambda > 450$ nm) for (a) 0–165 and (b) 0–30 min. Early in the course of reaction (b), the absorbances at 326 and 471 nm do not change (pseudoisosbestic points). However, at longer times the absorbances change at these wavelengths (a). The plot of the logarithm of absorbance at 580 nm vs time is shown in the inset in (b).

(7.7–9.6 ppm). Eventually the starting material is entirely consumed, and C continues to increase in concentration at the expense of B. Further irradiation leads to products D and E; however, their spectra were not fully resolved because of overlap with the spectrum of C. Moreover, shortly after B is consumed, precipitation occurs, preventing further monitoring of the reaction. At the point of precipitation, the NMR spectrum suggests that C is the major product in solution (60–80%), along with minor products E and F (Figure 4).⁴¹

In summary, we find that the ^1H NMR data are consistent with the overall sequential reaction $\text{A} \rightarrow \text{B} \rightarrow \text{C} \rightarrow \text{D} \rightarrow \text{E}$. The spectra suggest that these transformations are remarkably clean. However, the last two steps are difficult to characterize, owing to precipitation. Simultaneous monitoring of the UV–visible absorption spectrum of the NMR sample indicates that, at the point of precipitation, the products (mainly C) are essentially nonabsorbing between 400 and 800 nm. Thus, the UV–visible spectral changes are consistent with an $\text{A} \rightarrow \text{B} \rightarrow \text{C}$ type process. Moreover, the ^1H NMR spectra indicate that the first product (B) has C_s symmetry, whereas the second product (C) has the same (C_{2v}) symmetry as the starting

(41) It is clear that the ^1H NMR spectrum of D is composed of at least 10 resonances with equal integration (7.7–9.9 ppm). Product E appears to form after some build-up of D; the spectrum of E is characterized by at least five resonances with equal integration (7.3–8.8 ppm). The spectra are not inconsistent with E and F having C_s and C_{2v} symmetries, respectively.

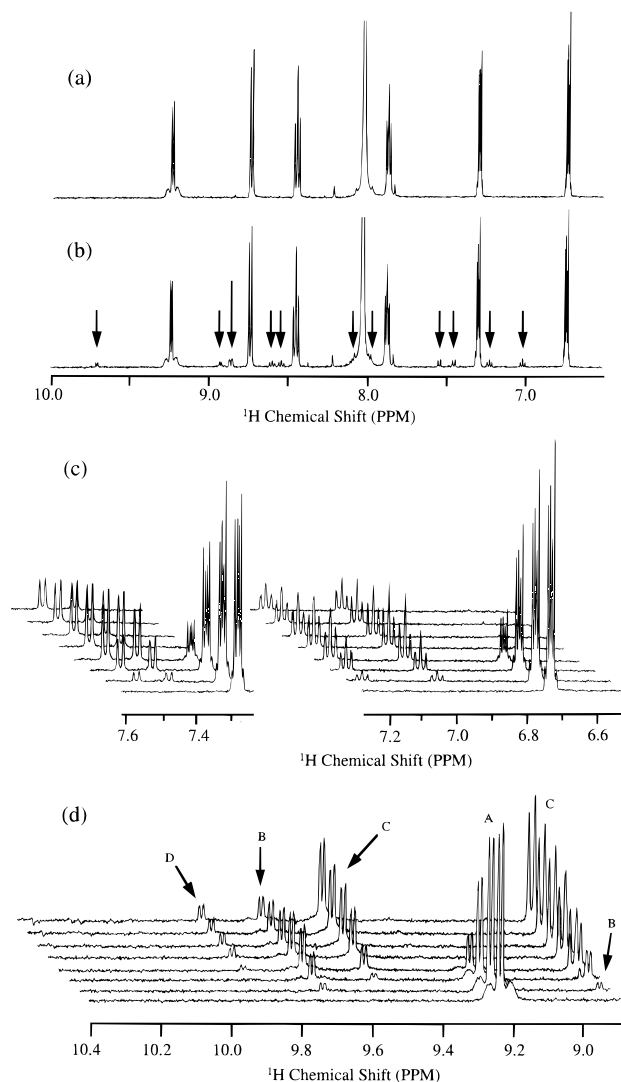


Figure 4. (a) ^1H NMR spectrum of Pt(bpy)(bdt) in $\text{DMF-}d_7$. Resonances at 7.83, 7.98, 8.01, 8.05, and 8.21 ppm also occur in the solvent blank. (b) ^1H NMR spectrum after 8 min of irradiation ($\lambda > 450$ nm). The 12 resonances corresponding to the C_s symmetric Pt(bpy)(bdtO₂) product are indicated with arrows. (c and d) Enlarged regions of ^1H NMR spectra recorded during the photooxidation reaction. In (c), the two resonances corresponding to Pt(bpy)(bdt) gradually lose intensity over time, whereas four resonances corresponding to Pt(bpy)(bdtO₂) emerge; at longer times, the latter resonances also lose intensity. In (d), resonances due to Pt(bpy)(bdt) (A), Pt(bpy)(bdtO₂) (B), Pt(bpy)(bdtO₄) (C), and an unidentified product, D, are observed. (Resonances corresponding to E do not appear in (a–d).)

Pt(bpy)(bdt) complex. Thus, these data are consistent with oxidation to form the C_s sulfinate and C_{2v} disulfinate products.

Photoproduct Structures. Our finding that the photoproducts B and C are less soluble than the starting material greatly aided in their characterization. For example, evaporation of a DMF solution of concentrated Pt(bpy)(bdt) exposed to air and room-light ($\lambda > 400$ nm) yielded an orange-yellow residue and small yellow crystals containing C. A single crystal selected for X-ray diffraction studies was found to be composed of water of crystallization and the disulfinate oxidation product, Pt(bpy)(bdtO₄), in which each sulfur is bonded to two oxygen atoms (Figure 5b). The ^1H NMR spectrum of the bulk material in $\text{DMSO-}d_6$ shows 6 resonances with equal integration (7.6–9.4 ppm). The spectrum of B is evident as the minor product (~15%).

In a similar experiment, evaporation of an acetonitrile solution of Pt(bpy)(bdt) exposed to air and room-light yielded yellow-

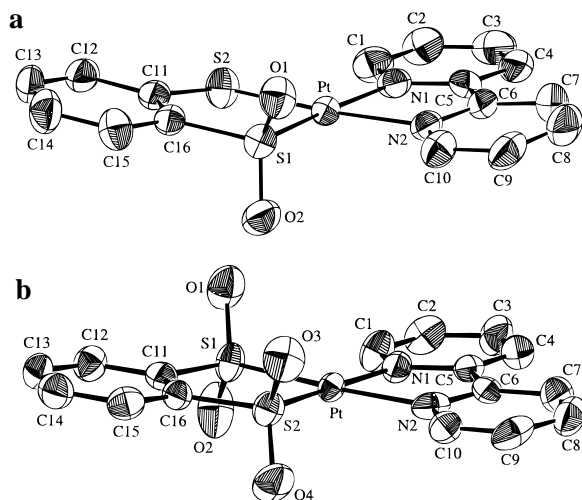


Figure 5. ORTEP diagrams with 50% probability ellipsoids showing the geometry of the photooxidation products (a) Pt(bpy)(bdtO₂) and (b) Pt(bpy)(bdtO₄). The disordered atoms, O3 and O4, bound to S2 are not shown in (a). H atoms are omitted for clarity.

orange crystals containing B. Presumably the lower solubility of the photoproducts in acetonitrile leads to precipitation of B before substantial further reaction to form Pt(bpy)(bdtO₄). A single crystal selected for X-ray analysis was found to be largely (86%) composed of the monosulfinate oxidation product, Pt(bpy)(bdtO₂), where two oxygen atoms have been added to one sulfur atom of the bdt ligand (Figure 5a), along with Pt(bpy)(bdtO₄) (14%). The C_s symmetry of the product is in agreement with our interpretation of the ¹H NMR and absorption spectra.⁴²

The distances and angles for the carbon atom framework of both Pt(bpy)(bdtO₄) and Pt(bpy)(bdtO₂) are normal. The Pt–S(sulfinate) bonds are short (2.22 Å), indicating a strong Pt–S interaction. The approximately tetrahedral geometry of the sulfinate S atoms and the 1.45 Å S–O bond lengths are in excellent agreement with structures of other transition metal sulfinate complexes.^{43–49}

Kinetics and Mechanism. We have monitored the initial photoreaction involving conversion of Pt(bpy)(bdt) to Pt(bpy)(bdtO₂) by observing changes in the UV–visible absorption spectrum during steady-state irradiation (λ_{ex} = 514 nm). Values for *k*_{obs} were determined from the negative slopes of linear fits to plots of the logarithm of absorbance as a function of irradiation time; only data collected during the decomposition of the first 15% of the starting material were fitted. For a given sample, the slopes are essentially invariant for measurements at wavelengths longer than 540 nm; that is, in the region where

(42) Since B must have C_s symmetry and O atoms bound to at least one sulfur, other possibilities include the monosulfenate/thiolate or the sulfenate/sulfinate adducts. The former cannot account for the observed electron density in the crystallographic data. In this regard, the latter is conceivable, though it presents mechanistic difficulties. Moreover, the absorption spectrum of B indicates that the CT still persists, albeit shifted to shorter wavelength (λ_{max} ~ 464 nm); thus, a more reasonable structure is one that retains a Pt–S(thiolate) bond.

(43) Nicholson, T.; Zubieta, J. *Inorg. Chem.* **1987**, *26*, 2094.

(44) Mirza, S. A.; Pressler, M. A.; Kumar, M.; Day, R. O.; Maroney, M. J. *Inorg. Chem.* **1993**, *32*, 977.

(45) Schrauzer, G. N.; Zhang, C.; Chadha, R. *Inorg. Chem.* **1990**, *29*, 4104.

(46) Dilworth, J. R.; Zheng, Y.; Lu, S.; Wu, S. L. *Trans. Met. Chem.* **1992**, *17*, 364.

(47) Farmer, P. J.; Solouki, T.; Mills, D. K.; Soma, T.; Russell, D. H.; Reibenspies, J. H.; Darensbourg, M. Y. *J. Am. Chem. Soc.* **1992**, *114*, 4601.

(48) Darensbourg, M. Y.; Tuntulani, T.; Reibenspies, J. H. *Inorg. Chem.* **1995**, *34*, 6287.

(49) Tuntulani, T.; Musie, G.; Reibenspies, J. H.; Darensbourg, M. Y. *Inorg. Chem.* **1995**, *34*, 6279.

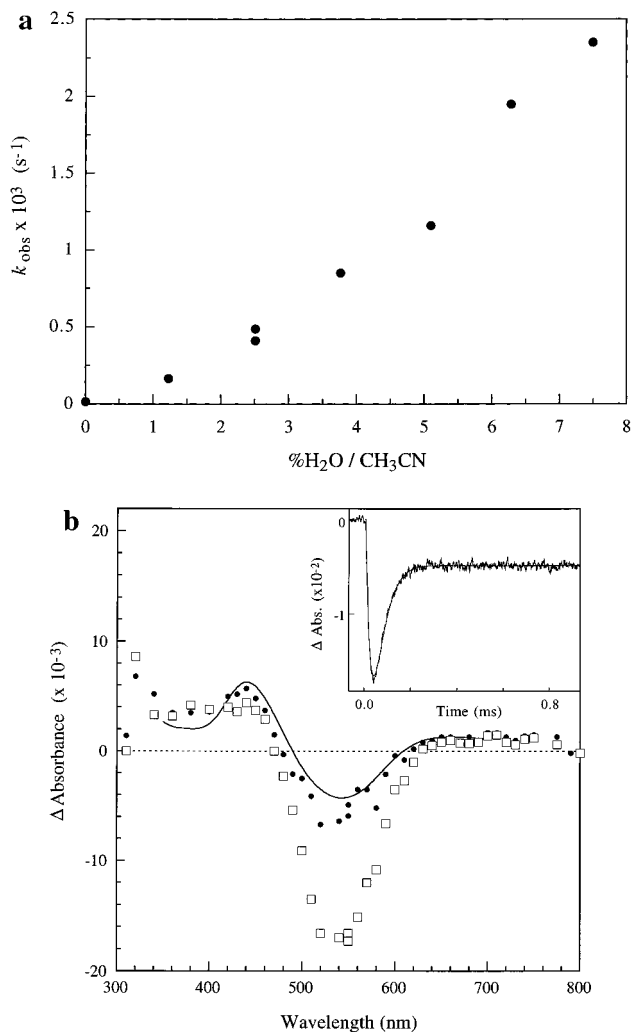
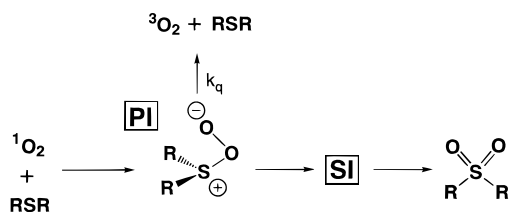


Figure 6. Observed pseudo-first-order initial rate constants (*k*_{obs}) for the steady-state photooxidation of Pt(bpy)(bdt) in aqueous CH₃CN as a function of %water content (λ_{obs} 580 nm, 15% depletion; λ_{ex} 514 nm, 0.01 mW). (b) Transient absorption spectrum of an air-saturated 0.1 mM Pt(bpy)(bdt) 10% H₂O/CH₃CN solution 40 μs (□) and 1 ms (●) after the excitation laser pulse (λ_{ex} 532 nm, 10 ns, 1 mJ). The solid curve corresponds to the difference absorption spectrum for Pt(bpy)(bdt) and {Pt(bpy)(bdt)}⁺ obtained by addition of 1 equiv of Ce⁴⁺ (2.5 mM Ce(NO₃)₄ in H₂O) to an acetonitrile solution. The inset shows the transient absorption kinetics at 550 nm following laser flash excitation (λ_{ex} 532 nm) of the air-saturated 0.1 mM Pt(bpy)(bdt) 10% H₂O/CH₃CN solution. The smooth line is the fit to the biexponential function C₀ + C₁e^{-k₁t} + C₂e^{-k₂t} (C₀, -4.9 × 10⁻³; C₁, 2.3 × 10⁻¹; C₂, -2.2 × 10⁻¹; k₁, 3.5 × 10⁴ s⁻¹; 2.8 × 10⁴ k₂, s⁻¹).

the products do not absorb. The rates are sensitive to water concentration, and reproducible results were obtained using acetonitrile/water mixtures of known concentrations (Figure 6a).

Under the conditions of our experiments, quenching to form the reactive oxygen species is very efficient; indeed, an O₂-saturated 2.5% H₂O/CH₃CN solution only reacts 25% more rapidly than an air-saturated solution. The strong water dependence is illustrated by the observation that *k*_{obs} for a 7.5% H₂O/CH₃CN (0.13 mM Pt(bpy)(bdt)) solution is approximately seven times greater than for a 1.23% H₂O/CH₃CN solution and 120 times greater than a ~0.01% H₂O/CH₃CN solution. Interestingly, the rate determined for the reaction in 2.5% D₂O/CH₃CN is indistinguishable from that determined for the reaction in 2.5% H₂O/CH₃CN. On the other hand, the reaction is dramatically accelerated in a deuterated acetonitrile solution (2.5% H₂O/2:1 CD₃CN:CH₃CN). This result is entirely consistent with the increased lifetime of singlet oxygen in deuterated

There also exists a close analogy between the singlet-oxygen reactivity of Pt(bpy)(bdt) and that of alkyl sulfides. The mechanism proposed by Foote and co-workers⁵⁹ for the latter process involves formation of two intermediates, **PI** and **SI**.



Though there is still considerable debate surrounding the details of this reaction,^{60–66} it is widely agreed that the zwitterionic persulfoxide, **PI**, is initially formed by reaction of the sulfide with ¹O₂. (A cyclic thiodioxorane or a hydroperoxysulfonium ylide (RS⁺(OOH)CH₂[−]) has been proposed as a possible secondary intermediate, **SI**.) In aprotic solvents, physical quenching dominates (>95%). However, in protic solvents (e.g., methanol or aqueous acetonitrile),⁶⁷ the sulfide oxidation is efficient, and no physical quenching is detected. In that case, the persulfoxide intermediate **PI** is proposed to be stabilized by hydrogen bonding or solvent addition to form a sulfuranium (e.g., R₂(OO)S–solvent⁺), thereby allowing for rearrangement to **SI**, which collapses to form products.

Recall that we also observe a dramatic acceleration in the rate of oxidation when water is added to an acetonitrile solution of Pt(bpy)(bdt), suggesting that a persulfoxide-type intermediate is formed in the Pt(bpy)(bdt) photooxidation reaction. Indeed, it is conceivable that a zwitterionic persulfoxide intermediate (or related adduct) is, in part, responsible for the transient absorption spectra obtained >1 μs after irradiation (Figure 6b), as such a species could have an absorption profile very much like that of {Pt(bpy)(bdt)}⁺.⁶⁸ To the best of our knowledge, the intermediates in the organosulfide reactions have not been directly observed.

We cannot rule out an oxygenation mechanism in which photogenerated ¹O₂ reacts with Pt(bpy)(bdt) to generate the oxidized complex and superoxide. That the excited-state complex does not appear to react directly to form a persulfoxide intermediate is compatible with the reduced nucleophilicity of the sulfur centers in the CT excited state. However, the surprising result is that O₂[−] is not generated in the initial excited-state quenching reaction, although there is clearly considerable driving force for this process: Pt(bpy)(bdt)* + ³O₂ → {Pt(bpy)(bdt)}⁺ + O₂[−], −ΔG° ~ 1.2 eV. One explanation is that the excited-state ET reaction is kinetically disfavored because it is highly inverted, whereas the subsequent conversion of ¹O₂ to

superoxide (or a persulfoxide species, by inference) has a much lower driving force (−ΔG° ~ 0.5 eV).⁶⁹

Experimental Section

Preparation of Pt(bpy)(bdt). In a typical procedure, 0.338 g of Pt(bpy)Cl₂ and 0.331 g of AgClO₄ were warmed in 25 mL of DMF (*N,N*-dimethylformamide, Burdick and Jackson) for 1 h. After cooling, the AgCl was removed by filtration through Celite, and a stoichiometric amount of 1,2-benzenedithiol with 2 equiv of NaOH_(aq) was added dropwise to the yellow filtrate. After several minutes, deep red needles of Pt(bpy)(bdt) formed in the intensely violet solution. The deep red-violet material can be recrystallized from acetonitrile. In the solid state, the compound is stable in the presence of air and light. ¹H NMR (DMSO) δ 6.71 (ddd, 1H, *J* = 5.9, 3.3, 0.5 Hz), 7.21 (ddd, 1H, *J* = 5.7, 3.4, 0.4 Hz), 7.78 (t, 1H, *J* = 6.6 Hz), 8.37 (t, 1H, *J* = 7.7 Hz), 8.65 (d, 1H, *J* = 8.0 Hz), 9.10 (d, 1H, *J* = 6.0 Hz). ¹H NMR (DMF) δ 6.73 (dd, 1H, *J* = 5.9, 3.2 Hz), 7.29 (dd, 1H, *J* = 5.8, 3.2 Hz), 7.86 (ddd, 1H, *J* = 6.9, 6.4, 1.3 Hz), 8.44 (dt, 1H, *J* = 1.4, 7.8 Hz), 8.73 (d, 1H, *J* = 8.1 Hz), 9.23 (d, 1H, *J* = 6.0, 0.6 Hz). Anal. (Calcd): C, 38.88 (39.10); 2.53 (2.46); 5.76 (5.70).

General Procedures and Instrumentation. ¹H NMR spectra were obtained using a Bruker AM500 spectrometer. UV–vis spectra were recorded using a Cary-14 spectrometer upgraded by OLIS to include computer control. Emission spectra were recorded using a system that has been described previously.^{70,71} Solution emission samples were freeze/pump/thaw cycled four times to give a final pressure of less than 10^{−5} Torr. Acetonitrile and dichloromethane were dried and distilled under argon or used as received from Burdick and Johnson.

Excitation pulses for solution emission lifetimes and transient absorption spectra⁷² were generated using a Quanta-Ray Nd:YAG laser (second harmonic, 532 nm). The pulse energy was attenuated to ~1 mJ using polarizers and monitored with a photodiode and discriminator. For transient absorption measurements, the probe light was provided by a PTI 75-W Xenon arc lamp operating in continuous-wave mode for long time scale measurements (≥1 ms) or pulsed-mode for short time scale measurements (≤1 ms). The emitted/transmitted light was passed through a monochromator prior to detection using a Hamamatsu 5-stage PMT. The signal was amplified using a Sony/Tektronix RTD 710 digitizer interfaced to an IBM PC.

Steady-State Photooxidation Studies. The reactions were monitored by absorption spectroscopy using a Hewlett-Packard diode array 8452A spectrometer; a 150 W tungsten lamp or the 514.5 nm line of an argon-ion laser attenuated to ≤0.01 mW were suitable excitation sources. Kinetics measurements were made using 3 mL samples of 1–2 mM aqueous acetonitrile solutions of known water content. The rates of photooxidation are strongly dependent on the presence of water. During the course of the reaction, the concentration of Pt(bpy)(bdt) was estimated from the absorbance at λ > 550 nm, where the photoproducts do not strongly absorb. Initial rates were determined from the slopes of linear fits of ln([Pt(bpy)(bdt)]) as a function of time up to 10–15% sample depletion; plots of ln([Pt(bpy)(bdt)]) vs time for >40% depletion are nonlinear.

Photooxidation of NMR samples was carried out using a 1000 W Hg/Xe lamp with a 450 nm cut-off filter and a water filter. The photooxidation products are readily identified by their ¹H NMR spectra: Pt(bpy)(bdtO₂) (DMF) δ 7.00 (ddd, 1H, *J* = 7.8, 7.1, 1.0 Hz), 7.22 (ddd, 1H, *J* = 7.9, 7.1, 1.3 Hz), 7.44 (dd, 1H, *J* = 7.6, 1.5 Hz), 7.53 (dd, 1H, *J* = 8.0, 1.0 Hz), 7.98 (ddd, 1H, *J* = 7.5, 6.8, 1.4 Hz), 8.08 (ddd, 1H, *J* = 7.3, 6.1, 1.4), 8.52 (dt, 1H, *J* = 1.5, 7.9 Hz), 8.58 (dt, 1H, *J* = 1.5, 7.8 Hz), 8.85 (d, 1H, *J* = 8.1; d, 1H, *J* = 8.2 Hz), 8.91 (d, 1H, *J* = 6.8 Hz), 9.70 (dt, 1H, *J* = 5.5, 0.6 Hz); Pt(bpy)-

(59) Liang, J.-J.; Gu, C.-L.; Kacher, M. L.; Foote, C. S. *J. Am. Chem. Soc.* **1983**, *105*, 4717.

(60) Watanabe, Y.; Kuriki, N.; Ishiguro, K.; Sawaki, Y. *J. Am. Chem. Soc.* **1991**, *113*, 2677.

(61) Jensen, F. *J. Org. Chem.* **1992**, *57*, 6478.

(62) Sheu, C.; Foote, C. S.; Gu, C.-L. *J. Am. Chem. Soc.* **1992**, *114*, 3015.

(63) Clennan, E. L.; Zhang, H. *J. Am. Chem. Soc.* **1995**, *117*, 4218.

(64) Clennan, E. L.; Dobrowolski, P.; Greer, A. *J. Am. Chem. Soc.* **1995**, *117*, 9800.

(65) Ishiguro, K.; Hayashi, M.; Sawaki, Y. *J. Am. Chem. Soc.* **1996**, *118*, 7265.

(66) Greer, A. C.; M. F.; Jensen, F.; Clennan, E. L. *J. Am. Chem. Soc.* **1997**, *119*, 4380.

(67) Oae, S. *Organic Sulfur Chemistry: Structure and Mechanism*; CRC Press: Boca Raton, FL, 1991; pp 465–470.

(68) There exists a similar analogy between the dehydrogenation reaction of **1** observed by Schanze and co-workers¹¹ and the α-proton exchange in alkyl sulfide reactions with singlet oxygen,⁶⁵ in the latter case, the persulfoxide intermediate is proposed to abstract an α-proton, giving a hydroperoxysulfonium ylide prior to formation of the sulfone product.

(69) We estimate E^{*+/−} for Pt(bpy)(bdt) to be ~1.7 V vs NHE and the reduction of molecular oxygen to occur at −0.47 V vs NHE in acetonitrile (e[−] + H⁺ + O₂ → [•]OOH, pH 7, 1:1 (Et₃NH)Cl/Et₃N in acetonitrile). The E_{0,0} for the lowest excited state of molecular oxygen (¹Δ_g) occurs at 1269 nm (0.98 eV). We also note that there is good overlap between the emission from Pt(bpy)(bdt) and the O₂ ¹Σ_g⁺ system (762 nm).

(70) Bailey, J. A.; Hill, M. G.; Marsh, R. E.; Miskowski, V. M.; Schaefer, W. P.; Gray, H. B. *Inorg. Chem.* **1995**, *34*, 4591.

(71) Rice, S. F.; Gray, H. B. *J. Am. Chem. Soc.* **1983**, *105*, 4571.

(72) Nocera, D. N.; Winkler, J. R.; Yocum, K. M.; Bordignon, E.; Gray, H. B. *J. Am. Chem. Soc.* **1984**, *106*, 5145.

Table 1. Crystallographic Data for Pt(bpy)(bdt), Pt(bpy)(bdtO₂), and Pt(bpy)(bdtO₄)·H₂O

	Pt(bpy)(bdt)	Pt(bpy)(bdtO ₂)	Pt(bpy)(bdtO ₄)·H ₂ O
formula	PtC ₁₆ H ₁₂ N ₂ S ₂	PtC ₁₆ H ₁₂ N ₂ S ₂ O _{2.28}	PtC ₁₆ H ₁₄ N ₂ S ₂ O ₅
<i>M_w</i> , g mol ⁻¹	491.49	527.96	573.50
color	violet	orange	yellow
crystal system	monoclinic	monoclinic	monoclinic
space group	<i>P</i> 2 ₁ / <i>n</i> (no. 14)	<i>P</i> 2 ₁ / <i>c</i> (no. 14)	<i>P</i> 2 ₁ / <i>c</i> (no. 14)
<i>a</i> , Å	8.206(2)	8.045(2)	11.513(2)
<i>b</i> , Å	11.456(4)	14.629(3)	7.103(1)
<i>c</i> , Å	16.350(4)	13.342(4)	20.856(3)
β, deg	103.14(2)	101.71(2)	101.64(1)
<i>V</i> , Å ³	1496.8(7)	1537.5(7)	1670.5(4)
ρ _{calc} , g/cm ³	2.18	2.28	2.28
<i>Z</i>	4	4	4
μ, cm ⁻¹	97.33	94.93	87.58
total no. of data ^a	5743	6125	6449
no. unique data	2634	2704	2943
no. parameters	190	228	235
GOF ^b	1.37	1.19	1.71
<i>R</i> ^c	0.033	0.034	0.055

^a All measured data were considered observed. ^b GOF = $(\sum w(F_o^2 - F_c^2)^2 / (n - p))^{1/2}$ where *n* is the number of data and *p* is the number of parameters refined. ^c *R* = $\sum |F_o - |F_c|| / \sum |F_o|$.

(bdtO₄) (DMF) δ 7.76 (dd, 1H, *J* = 6.0, 3.1 Hz), 7.95 (dd, 1H, *J* = 5.8, 3.0 Hz), 8.16 (ddd, 1H, *J* = 7.2, 6.4, 1.2), 8.62 (dt, 1H, *J* = 1.5, 7.8 Hz), 9.53 (ddd, 1H *J* = 5.5, 0.7, 0.7 Hz). Prolonged irradiation results in resonances corresponding to at least two additional products (D and E).

X-ray Crystallography. Diffraction data were collected at room temperature on an Enraf-Nonius CAD4 diffractometer (MoK_α radiation and graphite monochromator). Intensities were corrected for Lorentz and polarization effects. The intensities of three standard reflections showed no variations greater than those predicted by counting statistics. For each structure, the Pt coordinates were obtained from Patterson maps, and remaining non-hydrogen atom positions were determined from successive structure-factor, Fourier calculations. All non-hydrogen atoms were refined anisotropically. Ligand H atoms were positioned by calculation (C–H, 0.95 Å). Pertinent experimental data are collected in Table 1, and selected bond distances and angles are given in Table 2. In all cases, weights were taken as $1/\sigma^2(F_o^2)$; variances [$\sigma^2(F_o^2)$] were derived from counting statistics plus an additional term, $(0.014F_o^2)^2$; variances of the merged data were determined by propagation of esd's plus another additional term, $(0.014\langle F_o^2 \rangle)^2$. Atomic scattering factors were taken from Cromer and Waber.^{73,74} Computer programs used were those of the CRYM crystallographic computing system⁷⁵ and ORTEP⁷⁶.

Pt(bpy)(bdt). Needles suitable for crystallographic studies were grown in the presence of air by slow cooling of a hot DMF solution in the dark (3 days). (A crystal obtained by slow evaporation of an acetonitrile solution was found to have similar unit-cell dimensions.)

(73) Cromer, D. T.; Waber, J. T. In *International Tables For X-ray Crystallography*; Kynoch Press: Birmingham, 1974; Vol. IV, p 99.

(74) Cromer, D. T. In *International Tables For X-ray Crystallography*; Kynoch Press: Birmingham, 1974; Vol. IV, p 149.

(75) Duchamp, D. *Journal of the American Crystallographic Association Meeting*; Bozeman, MT, 1964; Paper B14, p 29.

(76) Johnson, C. K. *ORTEP*; Report ORNL-5138, Oak Ridge National Laboratory: Oak Ridge, TN, 1976.

Table 2. Selected bond lengths (Å) and angles (deg) for Pt(bpy)(bdt), Pt(bpy)(bdtO₂),^a and Pt(bpy)(bdtO₄)

	Pt(bpy)(bdt)	Pt(bpy)(bdtO ₂) ^a	Pt(bpy)(bdtO ₄)
Pt–S1	2.244 (2)	2.223 (1)	2.235 (3)
Pt–S2	2.250 (2)	2.256 (2)	2.218 (3)
Pt–N1	2.050 (4)	2.074 (4)	2.065 (8)
Pt–N2	2.049 (5)	2.075 (4)	2.076 (9)
S1–O1		1.460 (5)	1.462 (10)
S1–O2		1.442 (5)	1.430 (9)
S2–O3		1.272 (19)	1.455 (8)
S2–O4		1.605 (18)	1.467 (9)
S1–Pt–S2	89.0 (1)	88.8 (1)	88.9 (1)
N1–Pt–N2	80.1 (2)	78.6 (2)	79.3 (3)
O1–S1–O2		113.9 (3)	114.3 (5)
O3–S2–O4		115.9 (11)	112.4 (5)

^a For the structure of Pt(bpy)(bdtO₂), O1 and O2 have 92% occupancy, and O3 and O4 have 22% occupancy; the crystal contains 14% Pt(bpy)(bdtO₄).

A single crystal (0.26 × 0.18 × 0.15 mm) was mounted on a glass fiber; data (2 ≤ 2θ ≤ 50°; ±*h*, ±*k*, *l*) were corrected for absorption (Ψ-scan).

Pt(bpy)(bdtO₂). Crystals of the photooxidation products were obtained from air-saturated solutions of Pt(bpy)(bdt) left standing in room light. Under these conditions, the color of the solution gradually changes from violet to yellow and eventually becomes colorless. Because of their lower solubilities with respect to Pt(bpy)(bdt), the photoproducts have a tendency to precipitate from solution. In the case of Pt(bpy)(bdtO₂), an acetonitrile solution was allowed to evaporate to dryness, leaving orange crystals and residue. A single orange needle (0.50 × 0.06 × 0.05 mm) was mounted on a glass fiber; data (2 ≤ 2θ ≤ 50°; *h*, ±*k*, ±*l*) were corrected for absorption (Gaussian quadrature). The oxygen atoms O1 and O2 that are bound to S1 refined to 90% site occupancy; atoms O3 and O4 that are bound to S2 refined to 22% site occupancy. Since the UV–visible absorption and ¹H NMR spectra are consistent with a mixture of Pt(bpy)(bdtO₂) (B) and Pt(bpy)(bdtO₄) (C) in the bulk material, we have modeled the diffraction data as a mixture of both products.⁴² From the oxygen site occupancies, we find 84% Pt(bpy)(bdtO₂) and 14% Pt(bpy)(bdtO₄).

Pt(bpy)(bdtO₄)·H₂O. A yellow plate (1.0 × 0.5 × 0.2 mm) was selected from the crystals and residue obtained by evaporation of a DMF solution of Pt(bpy)(bdt) in room light. Data were corrected for absorption (Ψ-scan). The water oxygen OW is within H-bonding distance of O3 (2.95(1) Å) and O4 (2.92(1) Å), forming an O3–OW–O4 angle of 130.2(5)°; the water H atoms could not be located in the difference map.

Acknowledgment. We thank A. J. Di Bilio, M. G. Hill, L. M. Henling, V. M. Miskowski, and J. R. Winkler for expert technical assistance and helpful discussions. This work was supported by the National Science Foundation.

Supporting Information Available: Details of data collection and structure refinement and tables of atomic coordinates, bond distances and angles, anisotropic displacement parameters, and hydrogen atom positions for Pt(bpy)(bdt), Pt(bpy)(bdtO₂), and Pt(bpy)(bdtO₄) (26 pages). See any current masthead page for ordering and Internet access instructions.

JA9723803